

# Small-Angle X-ray Scattering on Two-Phase Systems under Pressure: Determination of Thermodynamic Parameters

M. Lorenzen,<sup>\*,†</sup> P. Bösecke,<sup>‡</sup> C. Ferrero,<sup>†</sup> C. Riekel,<sup>†</sup> and A. Eichler<sup>§</sup>

European Synchrotron Radiation Facility, B.P. 220, F-38043 Grenoble Cedex, France, MPG/ASMB c/o DESY, Gebäude 25b, Notkestrasse 85, D-22603 Hamburg, Germany, and Institut für Technische Physik, Mendelssohnstrasse 2, Technische Universität, D-38116 Braunschweig, Germany

Received November 19, 1996; Revised Manuscript Received July 14, 1997<sup>®</sup>

**ABSTRACT:** A small-angle X-ray scattering study on two different polyethylene samples under pressure up to about 750 MPa reveals a decrease of the Porod invariant  $Q(p)$  with increasing pressure at constant temperatures. The volume–pressure relationship as well as the isothermal compressibility and the Grüneisen parameter for a large pressure range and the overall density range are calculated from  $Q(p)$  with the help of the Tait equation. From the Porod invariant, the parameter  $B(t)$  of the Tait equation for the sample as well as of the purely amorphous and purely crystalline polyethylene are obtained. A general relationship between  $B(t)$  and the sample density has been found.

## 1. Introduction

High-pressure studies on polymers have been performed using various techniques, such as diffraction,<sup>1</sup> volume measurements,<sup>2–4</sup> and ultrasonic measurements.<sup>5</sup> However, small-angle X-ray scattering under pressure is a technique developed only recently, enabled by the construction of high-brilliance synchrotron sources.

The study of polymer systems with small-angle X-ray scattering (SAXS) can give an insight into the sample morphology. For two-phase systems, a parameter that is independent of the morphology—the Porod invariant  $Q$ —can be calculated. It relates the scattering curves to the volume fractions and the electron-density differences of the two phases.<sup>6</sup> In the case of a layered structure, the average thickness of the layers and their densities can be determined.<sup>7</sup> This information can then be correlated to molecular weight,<sup>7</sup> temperature,<sup>8</sup> thermal history,<sup>7</sup> degree of branching,<sup>8</sup> or pressure.

Polyethylene (PE) is an example of a two-phase system. Its morphology consists of lamellar phases: an amorphous and a crystalline one. Due to the electron density difference of these layers, Bragg scattering occurs in the small-angle scattering region, owing to the long period  $L$ , the distance between two layers of equal phase.

We study semicrystalline polyethylene under pressures up to about  $p = 750$  MPa at room temperature. In order to compare the small-angle scattering (SAXS) results with results from other experimental methods and theoretical predictions,<sup>9</sup> we have decided to derive some fundamental material features from SAXS data, like the relative change of specific volume  $v(p)$  as a function of pressure  $p$ . The latter has already been studied systematically on a large number of various polymers, e.g., by Zoller et al.<sup>10,11</sup> Thermodynamic properties such as the isothermal compressibility  $\kappa$  and the isothermal Grüneisen parameter  $\gamma$  can be derived once the change in volume is known.

The compressibility describes the response of a system to the external influence pressure change in the same

way as the thermal expansion coefficient  $\alpha$  describes the response to the external influence temperature change. In many materials applications it is necessary to know the volume changes with pressure and temperature and, thus, the compressibility and the thermal expansion.

The dimensionless Grüneisen parameter relates the macroscopic properties compressibility, thermal expansion, and specific heat to molecular motions. As can be deduced from different experimental methods such as measurements of sound velocity or volume changes, it can be regarded as a thermodynamic constant that links different experimental results.

## 2. Theoretical Section

**2.1. Tait Equation and Compressibility.** As the solid state of polymers is not a thermal equilibrium state, the dependence of the specific volume  $v$  on pressure  $p$  and temperature  $t$ , the  $vpt$  relationship, can only be represented by empirical relationships, for example, the Tait equation. It describes the variation of the volume with pressure at a constant temperature:<sup>12</sup>

$$v(p, t) = v(0, t)[1 - C \ln(1 + p/B(t))] \quad (1)$$

with:  $v(0, t)$  the specific sample volume at zero pressure,  $C$  a constant independent of pressure and material ( $C = 0.0894$ ), and  $t$  the temperature ( $^{\circ}\text{C}$ ).

The parameter  $B(t)$  (MPa) describes the influence of the temperature and is given by:<sup>12</sup>

$$B(t) = B_0 \exp(-B_1 t) \quad (2a)$$

However, for semicrystalline PE,  $B(t)$  can be approximated by a linear relationship:<sup>12</sup>

$$B(t) = B_0 + B_1 t \quad (2b)$$

The isothermal compressibility  $\kappa$  as a function of  $p$  and  $B(t)$  can be calculated from the Tait equation:

$$\kappa(p, B(t)) = -1/V[dV/dp]_t = C/[(p + B(t))(1 - C \ln(1 + p/B(t)))] \quad (3)$$

\* To whom correspondence should be addressed.

† European Synchrotron Radiation Facility.

‡ MPG/ASMB.

§ Institut für Technische Physik.

© Abstract published in *Advance ACS Abstracts*, September 15, 1997.

The compressibility is related to the isothermal Grüneisen parameter  $\gamma$ . The latter can be written as<sup>13</sup>

$$\gamma = -0.5[d \ln(1/\kappa)/d \ln V] \quad (4)$$

The compressibility can be approximately considered as a function only of the volume, which can be either affected by changes in temperature or pressure. In this case, (4) becomes<sup>13</sup>

$$\gamma = 0.5[d \ln(1/\kappa)/dp]_t \quad (5)$$

By inserting (3) into (5), one obtains the Grüneisen parameter as a function of  $p$  and  $B(t)$ :

$$\gamma(p, B(t)) = 0.5[1/C - \ln(1 + p/B(t)) - 1] \quad (6)$$

**2.2. The Porod Invariant.** In the case of small-angle scattering from an unoriented two-phase system, integrating the product  $I(q)q^2$  of the scattered intensity  $I(q)$  and the square of the scattering vector  $q$  ( $q = 4\pi/\lambda \sin \theta$ , where  $\lambda$  is the wavelength and  $\theta$  is the Bragg angle) over the whole  $q$  range, leads to the Porod invariant  $Q$ .  $Q$  relates the measured intensity to the sample composition, especially the volume fractions and electron densities:

$$Q(x_{v1}, x_{v2}, \rho_1, \rho_2) = 1/(2\pi^2) \int_0^\infty I(q) q^2 dq = (\rho_1 - \rho_2)^2 x_{v1} x_{v2} V_i \quad (7)$$

with  $\rho_1$  and  $\rho_2$  the electron densities of the two phases,  $x_{v1}$  and  $x_{v2}$  the volume fractions of the two phases, and  $V_i$  the illuminated volume.

In the case of polyethylene, the electron densities of both phases are proportional to the mass densities and can, therefore, be substituted by the mass densities,  $\rho_a$  and  $\rho_c$  ("a" stands for amorphous, "c" for crystalline). These are at ambient pressure:  $\rho_a = 855 \text{ kg/m}^3$  and  $\rho_c = 1000 \text{ kg/m}^3$ .<sup>14</sup>

The volume fractions of the purely amorphous and purely crystalline PE can be calculated from the mass densities of the sample  $\rho$ , the crystalline phase  $\rho_c$ , and the amorphous phase  $\rho_a$ :

$$x_{v1} = x_{va} = \rho(p, t)/\rho_a(p, t)[(\rho_c(p, t) - \rho(p, t))/(\rho_c(p, t) - \rho_a(p, t))] \quad (8a)$$

$$x_{v2} = x_{vc} = 1 - x_{va} \quad (8b)$$

Combining (7) with (8) leads to the Porod invariant, which is, thus, found to be dependent on pressure and temperature:

$$Q(p, t) \sim [\rho_a(p, t) - \rho_c(p, t)]^2 x_{va}(\rho_a(p, t), \rho_c(p, t), \rho(p, t)) x_{vc}(\rho_a(p, t), \rho_c(p, t), \rho(p, t)) \quad (9)$$

**2.3. The Porod Invariant Expressed in Terms of the Tait Parameter.** Shifting the reference pressure in eq 1 from zero to ambient pressure,  $p_0$ , and replacing volume by density, the Tait equation reads

$$\rho(p, t) = \rho(p_0, t)[1 - C \ln(1 + p_0/B(t))]/[1 - C \ln(1 + p/B(t))] \quad (10a)$$

**Table 1. Room Temperature Values of the Tait Parameter  $B(t)$  as a Function of Sample Density<sup>a</sup>**

$\rho$ (kg/m <sup>3</sup> )	$B(t)$ (MPa)	$p_{\max}$ (MPa)	$t$ (°C)	method	ref
855	162.5	0.1	21	from compressibility of purely amorphous PE	14
915	260	190	20	volume measurement	15
918.3	219	196	20	volume measurement	16
918.3	239.2	200	21	volume measurement	3
926.8	274.1	200	21	volume measurement	3
932.0	275.7	200	21	volume measurement	3
972.6	402.3	200	21	volume measurement	3
972.8	357.5	196	20	volume measurement	16
979.4	428.1	200	21	volume measurement	3
997	549.6	310	21.5	volume measurement	4
1000	466.1	300	20	diffraction	1
1000	513.7	0.1	21	from compressibility of purely crystalline PE	14

<sup>a</sup>  $p_{\max}$  is the maximum pressure to which the volume was measured or calculated.

For the limiting case of purely amorphous and purely crystalline material we write:

$$\rho_a(p, t) = \rho_a(p_0, t)[1 - C \ln(1 + p_0/B_a(t))]/[1 - C \ln(1 + p/B_a(t))] \quad (10b)$$

$$\rho_c(p, t) = \rho_c(p_0, t)[1 - C \ln(1 + p_0/B_c(t))]/[1 - C \ln(1 + p/B_c(t))] \quad (10c)$$

These equations can be used to replace density in eqs 8 and 9. Finally, we obtain the Porod invariant as a function of the Tait parameters  $B(t)$ ,  $B_a(t)$ , and  $B_c(t)$ .

### 3. The Tait Parameter and Its Relation to the Sample Density

In Table 1 literature values for the Tait parameter  $B(t)$  at room temperature are presented. Most of the values are either taken directly from the papers or computed by fitting the Tait equation to  $v(p)$  curves from the papers. The values of  $B(t)$  in the first and last row are calculated from the compressibilities of purely amorphous and purely crystalline PE at ambient pressure ( $\kappa_a = 5.5 \times 10^{-4} \text{ 1/MPa}$ ,  $\kappa_c = 1.6 \times 10^{-4} \text{ 1/MPa}$ )<sup>14</sup> using eq 3.

A least-squares fit to the data in Table 1 using a second-order polynomial

$$B(t = 21^\circ \text{C}, \rho) = \sum_{i=0}^2 a_i \rho^i \quad (11)$$

gives  $a_0 = 1.02 \times 10^4 \text{ MPa}$ ,  $a_1 = -23.9 \text{ (MPa} \cdot \text{m}^3)/\text{kg}$ , and  $a_2 = 1.42 \times 10^{-2} \text{ (MPa} \cdot \text{m}^6)/\text{kg}^2$  with a correlation coefficient  $R = 0.977$ . For polyethylene at room temperature (cf. Figure 1 broken line), the fitted polynomial describes the general relationship found<sup>17</sup> between the Tait parameter  $B$  and the density of the semicrystalline material fairly well.

The moderate correlation quality is mainly due to errors in the different experimental methods and to sample-to-sample variations of the densities  $\rho_a$  and  $\rho_c$ <sup>18,19</sup> as well as to differences in the PE samples (e.g., degree of branching and variety of side branches), which can cause differences in the compressibility of the samples. In addition, between the amorphous and crystalline layers interfacial layers exist with neither crystalline nor amorphous morphology. In our two-phase model they are not taken into account separately. However, their contribution to the sample density

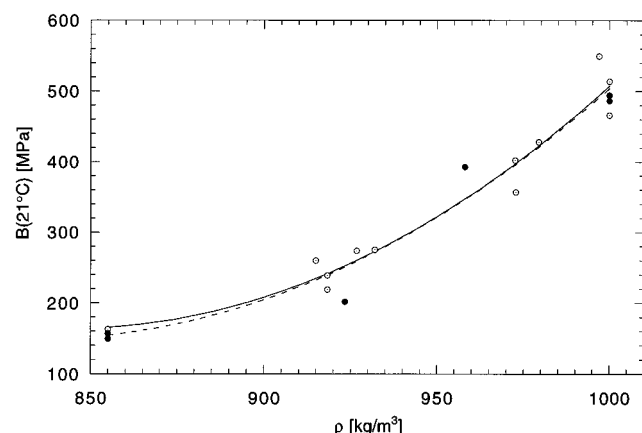


**Figure 1.** Room temperature values of the Tait parameter  $B$  vs mass density  $\rho$  for various PE samples: (empty circles) literature data (from Table 1); (full circles) own experimental results (from Table 3); (broken line) second order polynomial fit to the literature data (from Table 1); (full line) second order polynomial fit to all the data points (from Tables 1 and 3).

**Table 2. Physical and Chemical Parameters of the PE Samples<sup>a</sup>**

	LDPE	HDPE
$M_n^{28}$	14 000	13 600
$M_w/M_n^{28}$	5.37	3.87
degree of branching (CH <sub>3</sub> /1000 C)	24	0
density $\rho$ (kg/m <sup>3</sup> ) <sup>28</sup>	923.4	958.1
$x_{vc}$ (from density)	0.44	0.68
$T_s$ (°C) (peak temp)	106	131.5
long period $L$ (nm)	17.6	28.1
thickness (mm)	2.8	1.75
$T(13 \text{ keV})$ (%)	77.7	85.1

<sup>a</sup>  $M_n$  and  $M_w$  are the number and the weight averaged molecular weights,  $T_s$  is the melting temperature measured with DSC, and  $T$  is the transmission for X-rays.

influences the calculated crystallinity of the sample and, thus, gives rise to deviations between our model and the real sample.

In addition, the number of data points is not very high, especially in the low-density region. However, the temperature spread of  $\Delta t = 1.5$  °C between the different data points only leads to deviations of up to 0.5% in  $B(t, \rho)$  and can be neglected.

#### 4. Experimental Section

**4.1. Experimental Setup.** A detailed description of the pressure cell has been published previously.<sup>17,20</sup> In this cell solid and liquid samples can be pressurized to a maximum pressure of 1 GPa and heated to a maximum temperature of 300 °C.

The experiments have been performed at two different small-angle scattering stations (ID13 and ID2) at the ESRF<sup>21</sup> at 13 and 12.5 keV X-ray energies, respectively.<sup>22,23</sup> The detector-to-sample distance was 2.5 m. We used image plates<sup>24,25</sup> and gas-filled detectors<sup>26</sup> as two-dimensional detectors.

All data presented here are corrected for detector sensitivity and background scattering being due to the instrument and the pressure cell without sample.

**4.2. Samples.** Two PE samples of different crystallinities and degrees of branching have been studied: LDPE,<sup>27</sup> a low-density PE with side branches, and a high-density PE (HDPE) without side branches. The properties of both samples are given in Table 2.

At ambient pressure, they have been characterized by SAXS (see Figure 2a) and differential scanning calorimetry (DSC) (see Figure 2b). Comparing the widths of the Bragg reflections in Figure 2a, one can conclude that the distribution of the long

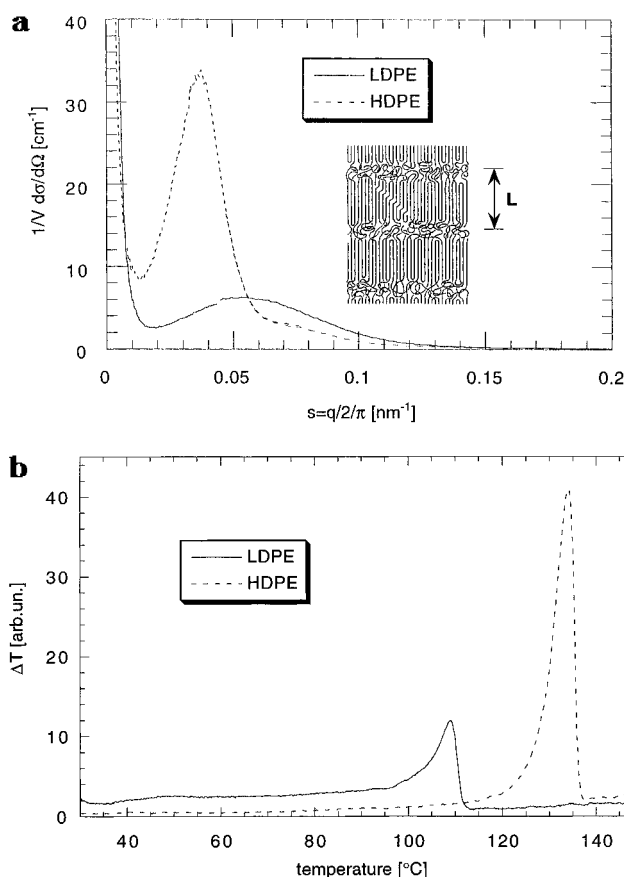


**Figure 2.** (a) Small-angle scattering from LDPE (full line) and HDPE (broken line) at ambient pressure. Inset: Morphology of polyethylene. (b) Differential scanning calorimetry curves for LDPE (full line) and HDPE (broken line) at ambient pressure.

periods  $L$  in the LDPE sample is wider than in the HDPE sample. From the positions of the maxima it can be seen that the long period of LDPE is smaller than that of HDPE. As can be seen in Figure 2b, the melting temperature of LDPE is lower than that of HDPE, which is due to thinner crystalline layers in the LDPE sample.

#### 5. Results and Discussion

Since all our experiments have been carried out at room temperature, from now on  $B(t = 21 \text{ °C}, \rho)$  will be referred to as  $B(\rho)$ ,  $B_a(t = 21 \text{ °C})$  as  $B_a$ , and  $B_c(t = 21 \text{ °C})$  as  $B_c$ .

**5.1. The Tait Parameter.** As an example, small-angle scattering curves of HDPE at some pressures are shown as a plot of  $I(s)s^2$  vs  $s$  in Figure 3 ( $s = q/2\pi = (2/\lambda) \sin \Theta$ ). These curves are integrated within the  $s$ -range shown in order to obtain the Porod invariant.

The experimental results regarding the Porod invariant at room temperature for HDPE and LDPE are given in Figure 4.

The lines in Figure 4 are obtained by means of a nonlinear least-squares optimization procedure for fitting eq 9 to the data points:  $B_a$  and  $B_c$  were first kept fixed to the values given by (11) and the fit parameter  $B(\rho)$  was obtained as a result. Then,  $B(\rho)$  was kept fixed and new values for  $B_a$  and  $B_c$  were found. This procedure was applied recursively and converged well after a few steps.

The results are given in Table 3. The standard deviation in  $B(\rho)$ ,  $B_a$ , and  $B_c$  due to the fit procedure is 0.078 for HDPE and 0.12 for LDPE.

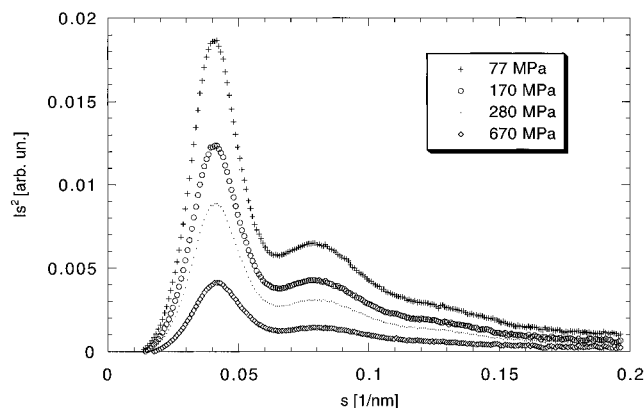


**Figure 3.** Small-angle scattering curves of HDPE at some pressures as a plot of  $I(s)s^2$  vs  $s$  ( $s = q/2\pi = (2/\lambda) \sin \Theta$ ).

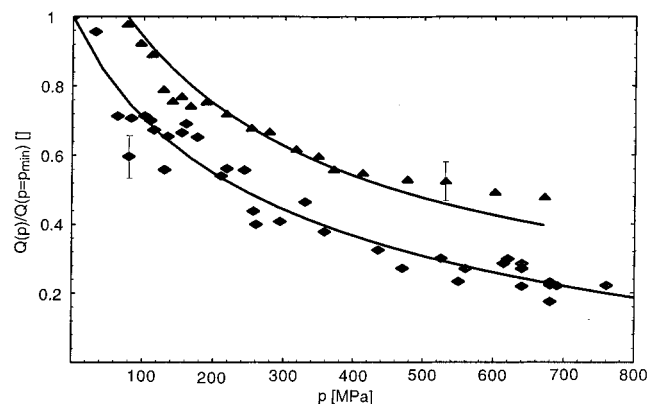


**Figure 4.** Relative Porod invariant  $Q$  of LDPE (lower curve) and HDPE (upper curve): (dots) experimental values; (full line) least-squares fit.

**Table 3. Tait Parameters at Room Temperature for the Two Polyethylene Samples of Different Density Obtained from the Fit Presented in Figure 4**

sample	density $\rho$ (kg/m <sup>3</sup> )	$B(21^\circ\text{C})$ (MPa)	$B_a(21^\circ\text{C})$ (MPa)	$B_c(21^\circ\text{C})$ (MPa)
LDPE	923.4	202.2	149.4	486.6
HDPE	958.1	393.1	156.7	494.2

The comparison of the results for  $B_a$  and  $B_c$  with literature data (see Figure 1 and Table 1) shows that our data lie well within the scatter of these data. The advantage of our new method for the determination of the Tait parameters  $B_a$  and  $B_c$  is that there is no need to study purely amorphous or crystalline material or to extrapolate from the properties of semicrystalline samples. However, with SAXS under pressure the properties of purely amorphous and purely crystalline material can be deduced directly from the study of a semicrystalline sample.

After having determined  $B(\rho)$ ,  $B_a$ , and  $B_c$  for PE at  $\rho = 923 \text{ kg/m}^3$  (sample LDPE) and  $\rho = 958 \text{ kg/m}^3$  (sample HDPE), the new values enlarge the data set presented in Table 1. In Figure 1, these new values are marked with filled circles. The fit of the enlarged data set (full line in Figure 1) yields the parameters  $a_0 = 9.25 \times 10^3 \text{ MPa}$ ,  $a_1 = -21.8 \text{ (MPa} \cdot \text{m}^3)/\text{kg}$ , and  $a_2 = 1.30 \times 10^{-2} \text{ (MPa} \cdot \text{m}^6)/\text{kg}^2$  with a correlation coefficient  $R = 0.979$ .

In addition to the effects discussed in section 3, the experimental error in the Porod invariant ( $\Delta Q = \pm 8\%$ ) leads to the observed scatter of our data points. However, our results confirm the general relationship found between the Tait parameter and the sample density of the literature values (see Figure 1).

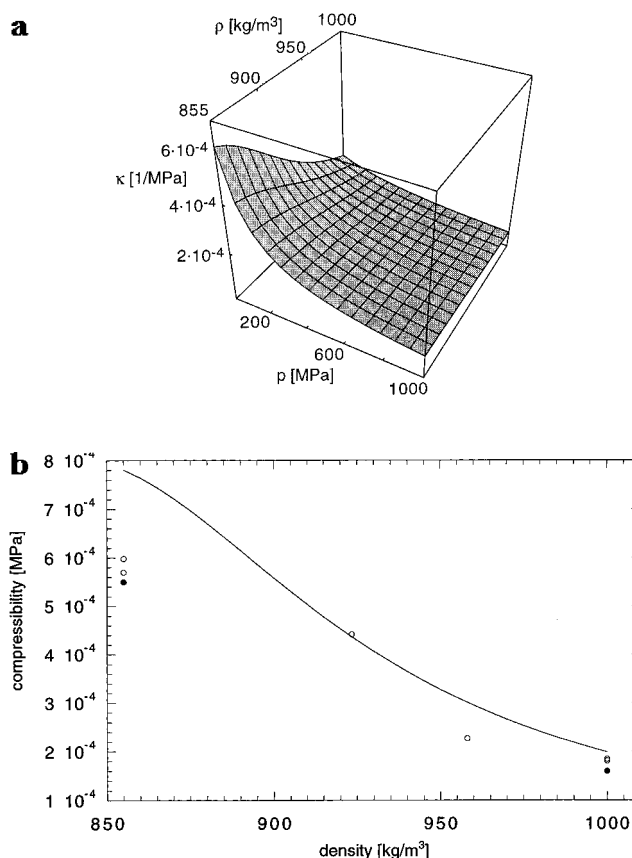


**Figure 5.** (a) Isothermal compressibility  $\kappa(p, \rho)$  of semicrystalline polyethylene as a function of pressure  $p$  and material density  $\rho$  (calculated with eq 3 and the fit to  $B(\rho)$  (full line in Figure 1)). (b) Section through the surface of Figure 5a at ambient pressure  $p_0$ . Full circles indicate literature data<sup>14</sup> for purely amorphous and purely crystalline PE, respectively. Empty circles indicate experimental results (calculated with eq 3 from the experimental results in Table 3).

**5.2. Compressibility and the Grüneisen Parameter.** Using the fitted  $B(\rho)$  curve and eq 3, the isothermal compressibility,  $\kappa(B(\rho), p)$  can be calculated for both the pressure range covered by the experiment and the whole density range of semicrystalline polyethylene (cf. Figure 1). Figure 5b shows the calculated compressibility  $\kappa(p_0, \rho)$  as a function of material density at ambient pressure  $p_0$  as well as the compressibility  $\kappa(\rho, B(\rho))$  for LDPE, HDPE, and purely amorphous and purely crystalline PE calculated with Tait parameters from Table 3. Literature data<sup>14</sup> for purely amorphous and purely crystalline PE are indicated for the sake of comparison.

The compressibilities of purely amorphous and purely crystalline PE agree well with the literature data except at low densities where a relatively large difference occurs between the calculated line and the literature data. This can be partly explained by the experimental and systematic errors in the Tait parameter, as discussed above. In addition, the compressibility at low densities is very sensitive to small variations in  $B(\rho)$  and literature values in this low-density region are lacking (compare with Table 1), which leads to uncertainties in  $B(\rho)$  at these densities. This fact is probably also responsible for the shape of  $\kappa(\rho)$  at low pressures and at low densities, which shows a smaller slope  $|d\kappa/d\rho|$  at low densities than expected (see Figure 5 a,b).

The pressure and density dependence of the Grüneisen parameter calculated with the aid of eq 4 is shown in Figure 6a. With increasing pressure  $\gamma$  decreases.

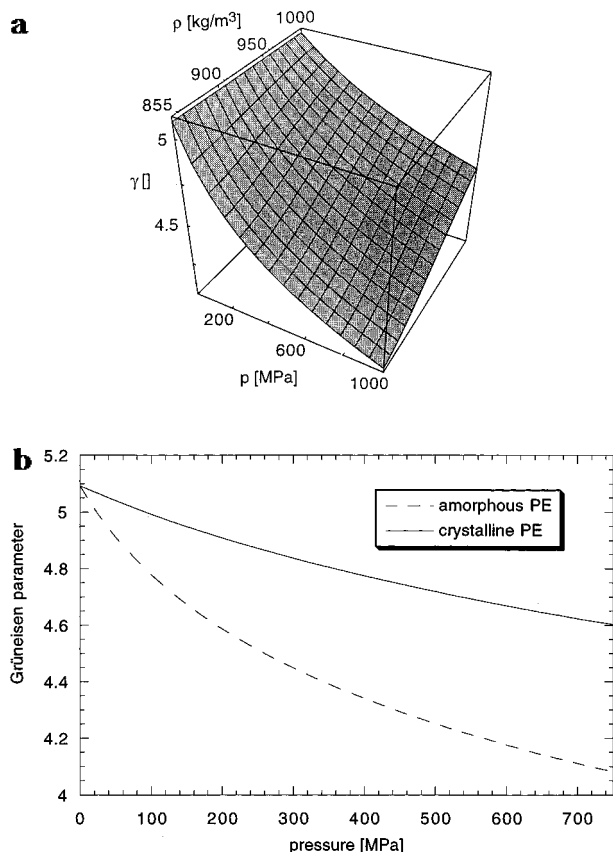


**Figure 6.** (a) Resulting Grüneisen parameter  $\gamma(p, \rho)$  of semicrystalline polyethylene as a function of pressure  $p$  and material density  $\rho$ . (b) Sections through the surface of Figure 6a at  $\rho = 855 \text{ kg/m}^3$  for purely amorphous PE and at  $\rho = 1000 \text{ kg/m}^3$  for purely crystalline PE.

This finding is consistent with the observations of Kijima<sup>5</sup> who studied the shape of  $\gamma_T$  (the adiabatic Grüneisen parameter derived from ultrasonic measurements) up to a pressure of 200 MPa.

At ambient pressure, the Grüneisen parameter calculated with (4) equals 5.1 for HDPE and LDPE. This value is in agreement with the results of ultrasonic ( $\gamma_T = 6-7$ ,<sup>5</sup>  $\gamma_T = 5.1$ <sup>13</sup>) and compressibility measurements ( $\gamma = 4.1$ <sup>13</sup>) and is independent of the sample density. However, the decrease of  $\gamma$  as a function of increasing pressure is not independent of density. At a pressure of 750 MPa,  $\gamma_a$  and  $\gamma_c$  show a difference of about 13% (see Figure 6b).

Using eq 4 or 5 for the calculation of the Grüneisen parameter yields the same results. This finding indicates that the compressibility  $\kappa$  of PE is a function of only the volume occupied by the material.

## 6. Summary

Small-angle X-ray scattering measurements under pressure have been performed on two different samples of semicrystalline polyethylene. A relationship between the Porod invariant  $Q(p)$ , measured as a function of pressure, and the Tait equation has been derived, by which the isothermal compressibilities and the Grüneisen parameter not only for the densities of both samples as well as of purely amorphous and purely crystalline PE but for the whole density range of polyethylene up to  $p = 750 \text{ MPa}$  were obtained. Considering the discussed errors, the results agree well with the values given in the literature.

With the presented method, besides the properties of the semicrystalline sample, the properties of purely

amorphous and purely crystalline material can be obtained from the same data set.

The relationship between the Tait parameter and sample density can be approximated by a second-order polynomial. This relationship is supported by the large amount of literature data found and the present SAXS measurements, even though more data especially from low-density samples are required in order to improve the quality of this statement.

The good agreement between the results obtained by application of this novel SAXS method and other experimental and theoretical findings shows that the pressure relationship of the compressibility and the Grüneisen parameter can be studied by small-angle X-ray scattering of pressurized samples.

## References and Notes

- (1) Ito, T.; Marui, H. *Polym. J.* **1971**, *2*, 768–782.
- (2) Sayre, J. A.; Swanson, S. R.; Boyd, R. H. *J. Polym. Sci., Polym. Phys. Ed.* **1978**, *16*, 1739–1759.
- (3) Olabisi, O.; Simha, R. *Macromolecules* **1975**, *8*, 206–210.
- (4) Kijima, T.; Koga, K.; Yoshizumi, T.; Imida, K.; Takayanagi, M. *Proceedings of the 4th International Conference on High Pressure*; The Physico-Chemical Society of Japan: Kyoto, 1974; pp 78–84.
- (5) Kijima, T.; Koga, K.; Imada, K.; Takayanagi, M. *Polym. J.* **1975**, *7*, 14–20.
- (6) Porod, G. In *Small-Angle X-ray Scattering*, 2nd ed.; Glatter, O., Kratky, O., Eds.; Academic Press: London, 1982.
- (7) Kortleve, G.; Vonk, C. G. *Kolloid Z. Z. Polym.* **1968**, *225*, 124–131.
- (8) Schouterden, P.; Vandermaliere, M.; Riekel, C.; Koch, M. H. J.; Groeninckx, G.; Reynaers, H. *Macromolecules* **1989**, *22*, 237–244.
- (9) Pastine, D. J. *J. Chem. Phys.* **1968**, *49*, 3012–3022.
- (10) Zoller, P. *J. Polym. Sci., Polym. Phys. Ed.* **1982**, *20*, 1453–1464.
- (11) Yi, Y. X.; Zoller, P. *J. Polym. Sci., Polym. Phys. Ed.* **1993**, *31*, 779–788.
- (12) Zoller, P. In *Polymer Handbook*, 3rd ed.; Brandrup, J., Immergut, E. H., Eds.; John Wiley and Sons: New York, 1989.
- (13) Hartmann, B. In *Proceedings of the 4th International Conference on High Pressure*; The Physico-Chemical Society of Japan: Kyoto, 1974; pp 111–114.
- (14) van Krevelen, D. W.; Hoftyzer, P. J. *Properties of Polymers*; Elsevier: Amsterdam, 1972.
- (15) Parks, W.; Richards, R. B. *Trans. Faraday Soc.* **1949**, *45*, 203–211.
- (16) Hellwege, K. H.; Knappe, W.; Lehmann, P. *Kolloid Z. Z. Polym.* **1962**, *183*, 110–120.
- (17) Lorenzen, M. *Small-angle scattering of X-rays by polymers under pressure*; Ph.D. Thesis, University of Braunschweig, 1995.
- (18) Swan, P. R. *J. Polym. Sci.* **1962**, *56*, 409–416.
- (19) Zachmann, H. G. In *Physik der Kunststoffe In Kunststoff-Handbuch*; Vieweg, R., Brown, D., Eds.; Carl Hanser Verlag: München, 1975; Vol. 1.
- (20) Lorenzen, M.; Riekel, C.; Eichler, A.; Häusermann, D. *J. Phys. IV C8* **1993**, *3*, 487–490.
- (21) European Synchrotron Radiation Facility.
- (22) Riekel, C.; Bösecke, P.; Diat, O.; Lorenzen, M.; Sanchez del Rio, M.; Snigireva, I. *Rev. Sci. Instrum.* **1995**, *66*, 987–994.
- (23) Bösecke, P.; Diat, O.; Rasmussen, B. *Rev. Sci. Instrum.* **1995**, *66*, 1636–1638.
- (24) Svensson, O. Characterization and Calibration of an Imaging Plate Detector for Use in Synchrotron Radiation Crystallography. Licentiate Thesis, University of Göteborg, 1994.
- (25) Kodak plates with Molecular Dynamics 400E scanner.
- (26) Berry, A.; Gabriel, A.; Kocsis, M.; Riekel, C. *Nucl. Instrum. Methods Phys. Res.* **1994**, *A348*, 334–337.
- (27) Lupolen, Trademark of BASF.
- (28) Measured by U. Dambeck, and B. Ossenbrüggen, Institut für Technische Makromolekularchemie (TMC), Hamburg, Germany.